Effects of ausforming temperature on carbide-free bainite transformation and its correlation to the transformation plasticity strain in a medium C- Si-rich steel

M. Zorgani, C. Garcia-Mateo, M. Jahazi

Article published in journal of Materials Characterization, 111124, Volume 176, April 2021.

The final publication is available at DOI:10.1016/j.matchar.2021.111124

Effects of ausforming temperature on carbide-free bainite transformation and its correlation to the transformation plasticity strain in a medium C- Si-rich steel

M. Zorgani[1*], C. Garcia-Mateo[2], M. Jahazi[1*]

1 Department of Mechanical Engineering, École de Technologie Supérieure, 1100 Notre-Dame Street West, Montreal, QC, Canada H3C 1K3

2 National Canter for Metallurgical Research (CENIM-CSIC), Avda. Gregorio del Amo 8, Madrid *28040, Spain*

Abstract

Ausforming treatments at different temperatures were applied to a medium C-Si rich carbide free bainitic steel, and the role of transformation plasticity on the evolution of the microstructure is discussed. Three ausforming temperatures were selected prior to isothermal bainite transformation at 325 ^{o}C. Deformation was applied above the bainite start temperature, B_S, (600 ^{o}C), below B_S (400 ^{o}C), and at the isothermal transformation temperature (325 ^{o}C). A combination of high-resolution dilatometry, XRD, SEM, and EBSD was used to investigate phase changes, microstructure evolution, and variant selections for the different ausforming conditions. The results indicated that the transformation rate was enhanced for all deformation conditions compared with the pure isothermal condition. Ausforming above B_S did not modify the morphology of the carbide free microstructure, while ausforming below B_S led to an asymmetrical morphology in the specimen. The alignment of the bainite plates can be at a random or a specific angle, depending on the supercooled austenite condition prior to the bainitic transformation. The thickness of the bainitic ferrite plates was refined to about 100 nm for the ausforming cycle at 325 ^{o}C resulting in a hardness of values of 540 HV. Transformation plasticity strains increased with increasing bainite transformation and were more intense with increasing microstructure alignment at the two lower ausforming temperatures. Texture studies revealed that both pure isothermal and ausforming at temperatures above B_S resulted in an almost random texture, while a strong texture was obtained when ausforming below B_S, a which was attributed to variant selection.

Keywords: Ausforming; Carbide-Free Bainite; Transformation plasticity; microstructure alignment

1 Introduction

Deforming metastable austenite followed by bainite transformation, also termed ausforming, is an alternative way to modify carbide-free-bainite (CFB) morphology to a nanostructure in medium and low carbon steels. The pre-straining is usually applied in the bay between the ferrite/pearlite and bainite curves of the time-temperature-transformation (TTT) diagram, or it can be done at lower temperatures, between the bainite start temperature (B_S) and martensite start temperature (M_S). The nanostructured bainitic microstructure has been produced in medium-carbon Si-rich alloy steels by applying deformation in the 600-300 ^oC temperature interval, followed by an isothermal transformation at a temperature close to M_S [1-7]. In addition to altering the morphology, ausforming can enhance the transformation kinetics and, in some cases, the amount of transformed bainite [8]. The incubation and transformation times are shortened as the pre-deformation temperature is reduced [9, 10].

Displacive transformations, such as martensite and bainite, are always associated with a shape deformation that encompasses a significant shear component ($s\approx0.26$) and small dilatation strain ($\delta\approx0.03$) as a result of the invariant plane strain (IPS) [11, 12]. Due to the IPS, the volume change is always assumed to be isotropic when the bainitic reaction occurs without influences of other factors (e.g., external superimposed stress and/or deformation before transformation) [13-15]. The transformed bainite commonly has a Kurdjumov-Sachs, K-S, orientation relationship with the parent austenite, where 24 variants could be grown in one austenite grain [16-18]. However, when the bainite plates grow in a specific/preferred orientation, the transformation is considered anisotropic, and therefore the volume change could not be assumed identical in all directions. The anisotropy in volume change during bainite transformation could be described in terms of transformation plasticity (TP) or, in other words, the strain associated with the anisotropic bainitic transformation. It has been reported that an increase in nucleation and growth of bainite subunits intensified the TP strains [13, 14, 16, 19], and therefore, TP strain could be used to quantify the influence of process parameters on the level of anisotropy in bainitic transformation.

Magee [20] and Greenwood-Johnson [21] proposed models describing the evolution of TP strains. The former explained that the increase in TP strains could be due to an alignment in the martensite or bainite variants in specific directions and angles. The author referred that to the additional mechanical driving force due to the applied stresses that promote specific variants to grow faster than others during bainitic and martensitic transformation. Greenwood-Johnson linked the evolution of the TP strains to the volumetric difference between the austenite and the bainite or martensite phases due to the micro deformations that occur in the weaker phase, i.e., austenite [22, 23]. Han et al. and Liu et al. [16, 24] in their work provided supporting evidence that in the case of low carbon steels, the evolution of TP strain followed the Greenwood-Johnson model while Rees et al. and Uslu et al. [25, 26] reported that in medium carbon steels the evolution of TP strain was according to the Megge model. Note that in the studies mentioned above, the bainitic transformation took place under the influence of applied stress.

Recently Liu et al. [14] investigated the effect of plastic stress applied during bainite transformation at different temperatures on the evolution of TP strains in a CFB steel with medium C content. The authors concluded that the development of the TP strain was compatible with the Magee mechanism. Their results showed that the TP strain slightly increased when the stress was *below* the yield strength of the parent phase (i.e., austenite), while the TP increased remarkably if the applied stress was *above* austenite yield stress (i.e., austenite was plastically deformed). In contrast, Zhou et al. reported a strong variant selection (i.e., high TP values) in the microstructure when the applied stress was *below* austenite yield strength [27]. Furthermore, the impact of the pre-deformation temperature prior to the bainitic reaction was not investigated in the above studies.

Lambers et al. [15] reported that TP strains altered and increased with applied external stresses, whether below or above the austenite yield stress, during bainitic transformation in a low-alloy 51CrV4 steel. The authors found that changes in the TP strain evolution were initiated during the pre-straining stage of the supercooled austenite prior to transformation. The changes in the TP strain reached a steady state when the deformation level reached about 3% for all conditions. Such changes were associated with the crystallographic texture in the deformed austenite and the invariant-plane strain shape

accompanying the displacive growth [13]. The authors also found that the enhancement of the bainite transformation, due to the plastic pre-deformations, generated more residual stresses in the supercooled austenite and increased the TP strains. In another study conducted on the same steel [28], the author found that the TP strain was reduced when a 4% pre-strain temperature increased by 100 ^{o}C, from 400 ^{o}C to 500 ^{o}C. Note that in these studies, the pre-deformation amount was only 6.5% at 1050 ^{o}C and 3% at 340 ^{o}C, which are quite low values to be able to determine a clear and quantifiable trend.

The present work is defined in this context and has for objective to investigate the effect of the compressive plastic deformation temperature on the CFB transformation in terms of microstructural and kinetic behavior and their relation to the evolution of TP strains during the bainitic transformation in medium-carbon CFB steel. The temperatures and deformation levels were selected to allow for quantification of the impact of TP strain and a clear distinction of the role of variant selection in the transformation process.

2 Material and experimental procedure

A medium C-high Si steel was used in this study, and its nominal chemical composition is shown in Table 1. The presence of Mn and Cr enhances the steel hardenability and makes it suitable to perform the ausforming process, and Mo also can increase the hardenability and prevent temper embrittlement [29]. Silicon (Si) is typically added to suppress cementite precipitation during the bainitic reaction [30].

Table 1 Chemical composition of the steel studied in wt. %.

C	Si	Mn	Cr	Mo	Fe
0.4	1.7	1.5	1.5	0.4	Balance

The thermal and thermomechanical treatments, with and without deformation, were performed in a high-resolution deformation dilatometer (DIL805A/D-TA) using a particular module for thermomechanical treatments. For this purpose, cylindrical specimens 10 mm in length and 5 mm in diameter were used for both pure isothermal and ausforming tests. Molybdenum discs were spot welded on specimen sides to reduce the

friction between the specimen and the silicon nitride (Si_3N_4) stamps during the deformation step and ensure a uniform distribution of temperature along the specimen during the thermomechanical process.

For controlling the temperature cycle, a type-K thermocouple was welded in the middle of the specimen, where the variation along the specimen length was ±5 ºC. **Error! Reference source not found.**a and 1b are the schematic description of the dilatometry used in this study.

The thermal and thermomechanical cycles are schematically illustrated in Figure 1**Error! Reference source not found.**c, and further details on the selection of the conditions can be found in ref. [31]. Specimens were heated at 10 $°Cs^{-1}$ to a temperature of 980 °C, where they were held for 5 min under vacuum. They were then cooled at 20 $°Cs^{-1}$ to the three selected deformation temperatures, where a 20% deformation at a deformation rate of $1mms^{-1}$ was applied. Considering that bainite and martensite start temperatures (B_S and M_S) of the steel were determined to be 470±10 and 310±5 ºC, respectively, and the bay between ferrite/pearlite and bainite (F/P-B) delimited between 500-600 ºC [31].

Deformation temperatures (T_{def}) prior to isothermal transformation at 325 °C (T_{Iso}) were selected as follows: i) $T_{def} > B_S$ at 600 °C; ii) $B_S > T_{def} > T_{Iso}$ at 400 ºC; and iii) $T_{def} = T_{Iso}$ at 325 °C. The deformation step was selected to be less than 10 s to avoid possible bainite transformation during the deformation process [31]. The deformed samples were cooled down to T_{Iso} = 325 °C at a cooling rate of 20 °C/s and then held for 30 min to allow the bainitic transformation to finish. For comparison purposes, a pure isothermal test at 325 ºC (with no previous deformation) was also carried out under the same conditions as the ausformed specimens. It must be noted that no other phase transformations were detected by dilatometry prior to deformation or during cooling to the isothermal transformation stage, indicating that the microstructure is fully austenitic in all cases prior to the bainitic transformation. Moreover, no martensitic transformation was detected on cooling to room temperature after isothermal holding time.

In order to accurately determine the bainitic transformation's kinetics, diametrical and longitudinal dilatations were recorded to calculate the Relative Change in Volume (RCV) of each specimen. The Relative Change in Length (RCL) was recorded using a Linear Variable Differential Transducer (LVDT), while the Relative Change in Diameter (RCD) was measured using a laser scanning system that automatically locates itself at the specimen's mid-length regardless of deformation. It should be noted that the RCL and RCD dilatometric signals were recorded simultaneously during bainitic transformation. The amount of expansion obtained from the dilatometer, whether longitudinal or diametrical, was normalized by dividing the instantaneous dilatation of the specimen length or diameter before the transformation. As anticipated, for consistency, all the treatments were performed on the specific *deformation* module of the DIL 805 dilatometer, where a minimal load of the order of 4 MPa is applied to hold the specimen.

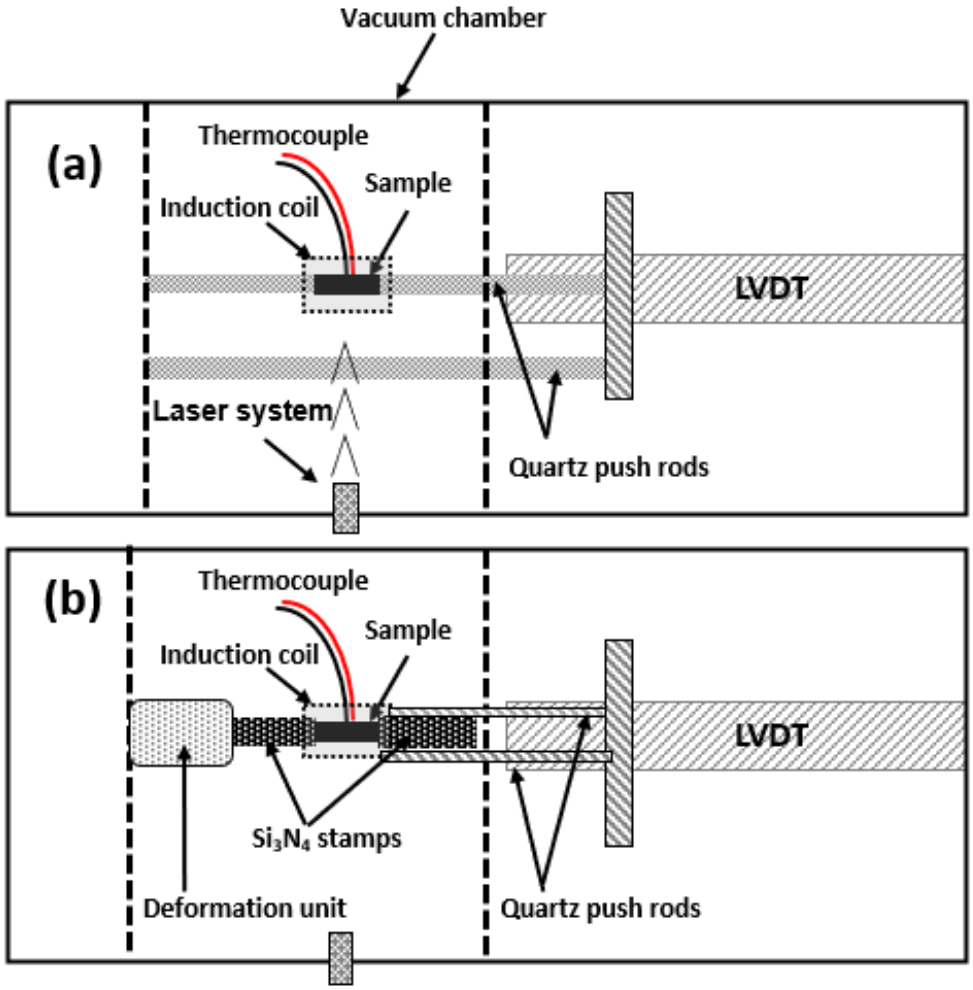

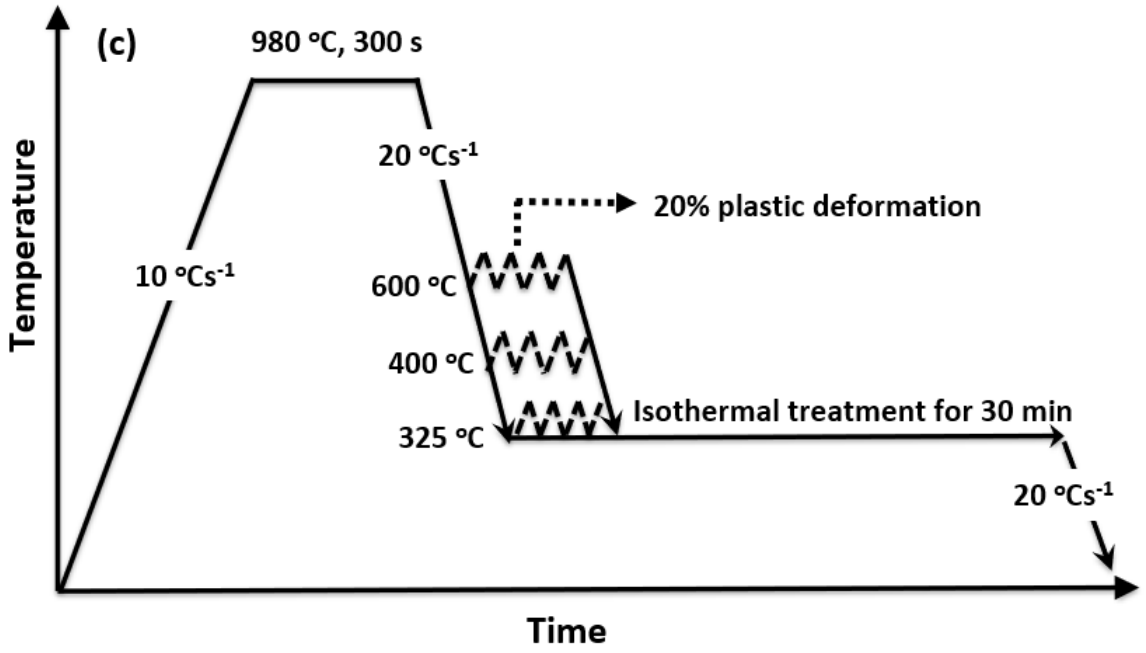

Figure 1 Dilatometry set up for two used modules (a) quenching; (b) deformation; (c) pure isothermal and ausforming experimental procedures.

Microstructural characterization was carried out on both longitudinal (L) and transverse (T) sections of the tested specimens using optical and Scanning Electron Microscopy (SEM). Specimens for SEM investigations were prepared according to standard metallography procedures. After the final polishing step was completed, a cycle of etching (3 % Nital for 5 s) and polishing with 1µm cloth was implemented to remove the deformed layer formed during the grinding process, ending with an etching step for SEM examination.

Measurements of the bainite plate thickness were done in the longitudinal ($t_{L\alpha b}$) and transverse ($t_{T\alpha b}$) sections by using the linear intercept (l_i) method in a direction normal to the plate length. Four SEM frame images were taken for each specimen to determine the bainite plates thickness, with 50 measurements for each frame (total of 200 measurements for each condition), and a stereological correction factor ($t_{\alpha b}$=2 (l_i) /π) was applied [32] to obtain the actual plate thickness. Electron backscattered diffraction (EBSD) analysis was

conducted using a Bruker e-Flash HR EBSD detector mounted on a Field Emission SU8230 Hitachi SEM. The orientation data were analyzed using the non-commercial orientation imaging software ATEX. [33]. The EBSD specimens were prepared in the same way as SEM imaging specimens plus a final preparation step with a colloidal silica solution to clean the specimens and remove any deformed sub-layer from the studied surface. The volume fraction of the blocky-shape retained austenite (RA_{block}) was estimated using the EBSD phase-detection method. The RA_{block} larger than 100 nm were considered as blocky-shape retained austenite; otherwise, the remainder was considered film-like austenite (RA_{film}). Two maps with an area of 800 μm^2 with a step size of 50 nm were used to obtain the average amount of RA_{block}.

The total amount of retained austenite ($RA_T = RA_{block} + RA_{film}$) was measured using X-ray diffractometer (X'PERT PANalytical) with Co Kα radiation by means of the direct comparison method [34]. All XRD specimens were prepared using a method similar to that used for metallographic assessment. The acceleration voltage was 45 kV with a scan range of 2θ from 40 to 120^o, with a step size of 0.05°. Four integrated intensities were used to reduce the influence of crystallographic texture, as reported in previous studies [34, 35]. For austenite, (111), (200), (220), and (311) peaks; and for ferrite (110), (200), (211), and (220) peaks were examined. Two specimens were tested for each condition for repeatability purposes.

Hardness measurements were conducted using a Vickers hardness tester with a 10 kilogram-force (kgf) and a dwell time of 15 s. The 10 Kgf load was chosen to reduce the load sensitive effect due to expected fine features. The reported hardness values on each section of the specimen corresponding to an average of three indentations.

3 Results and discussion

3.1 Dilatation behavior during bainitic transformation

Figure 2 shows the RCL and RCD behavior during the isothermal transformation at 325 ^{o}C for the pure isothermal (Iso) and ausformed conditions at the three deformation temperatures, at 600 ^{o}C (Def_600), 400 ^{o}C (Def_400), and 325 ^{o}C (Def_325).

As shown in Figure 2a, the dilatation behavior in the non-ausformed (Iso) sample is very similar in both RCL and RCD directions and largely overlap each other, suggesting a random growth of the bainite plates in different direction. Such growth has been called isotropic by some authors [36, 37] . A nearly similar behavior is observed for the Def_600 sample with slight difference between RCL and RCD singles (Figure 2b) revealing that high temperature ausforming results in an isotropic development of bainitic plates like those in Iso condition.

In contrast, for the low deformation conditions (< BS) the dilatation diverged into two opposite directions. Specifically, while a contraction was observed in the RCL signal for Def_400 and Def_325 specimens, RCD curves showed an expansion (Figure 2c and 2d). The above observed anisotropy in the dilatometric behavior could be analyzed in terms of preferred orientation of bainite plates and a stronger or weaker variant selection which assist their growth as will be discussed further in the manuscript [36, 37]

As shown in Figure 2a (blue lines), slight variations are present in the RCL and RCD signals for the pure isothermal test. In order to validate whether this variation was material or equipment related, a validation test was conducted for the pure isothermal condition by utilizing the *quench module* of the dilatometer (i.e., the slight pressure that is applied on the specimen when the *deformation module* is used was eliminated). Figure 2a (blue lines) shows that the RCL curve coincided with the RCD curve, indicating that the slight variations were due to the small load to hold the specimen. This experiment also revealed that the shape of the RCD curves was almost identical for both modules; therefore, and for the sake of higher accuracy, the analysis of the data will be based on the evolution of the RCD values.

The RCD signals in Figure 2 indicate that the incubation time was shortened when the ausforming was conducted at 600 ^{o}C (Def_600) compared with the pure isothermal condition, although the maximum RCD dilatation was almost equal in both situations. However, the incubation time was barely seen for the low-temperature ausforming conditions (Def_400 and Def_325). Specifically, compared to the Iso specimen, radial expansion (RCD) increased by about 60 and 70 % in Def_400 and Def_325 specimens.

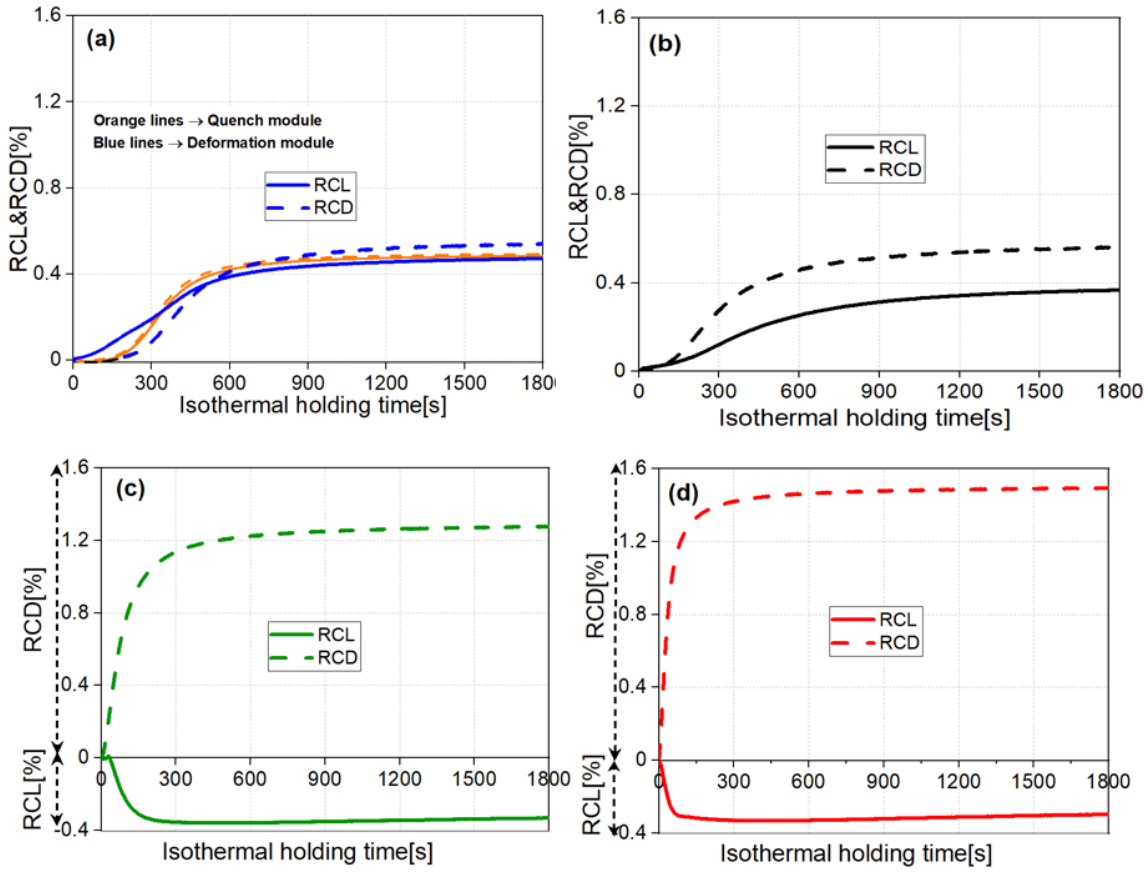

Figure 2 RCL and RCD. versus transformation time for all experimental conditions: (a) Iso, (b, c, and d) Def_600, Def_400, and Def_325, respectively (The solid and dashed lines stand for RCL and RCD).

By means of the derivate of the RCD (dRCD/dt), the kinetics of the bainitic transformation can be depicted in more detail. The values above each peak in Figure 3 represent the relevant time intervals for reaching the maximum transformation rate for each condition. As shown in Figure 3, when transformation starts almost immediately at the isothermal temperature, and the vast majority of the transformation occurs in a very short time, Def_400 and Def_325 in Figure 2 and Figure 3, the dRCD/dt peaks are high and narrow.

On the other hand, if transformation requires an incubation time to start and then progressively occurs during a longer span of time, the resulting dRCD/dt peaks are shorter and broader, as in Iso and Def_600 conditions.

The observed significant increase in the RCD and dRCD/dt of the low-temperature deformed specimens could be related to the increase in the number of nucleation sites for bainite as a result of deformation. Hu et al. [10], Shipway et al. [38], and Gong et al. [39] reported that defects such as dislocations, twins, and grain boundaries generated by deformation prior to transformation act as bainite nucleation sites. Specifically, Gong et al. [39], using a 3D-SEM technique, reported that pre-existence bainitic ferrite plate acted as a nucleation site for secondary bainite plate in case of ausforming, thereby enhancing the bainite transformation, especially at the beginning of the transformation.

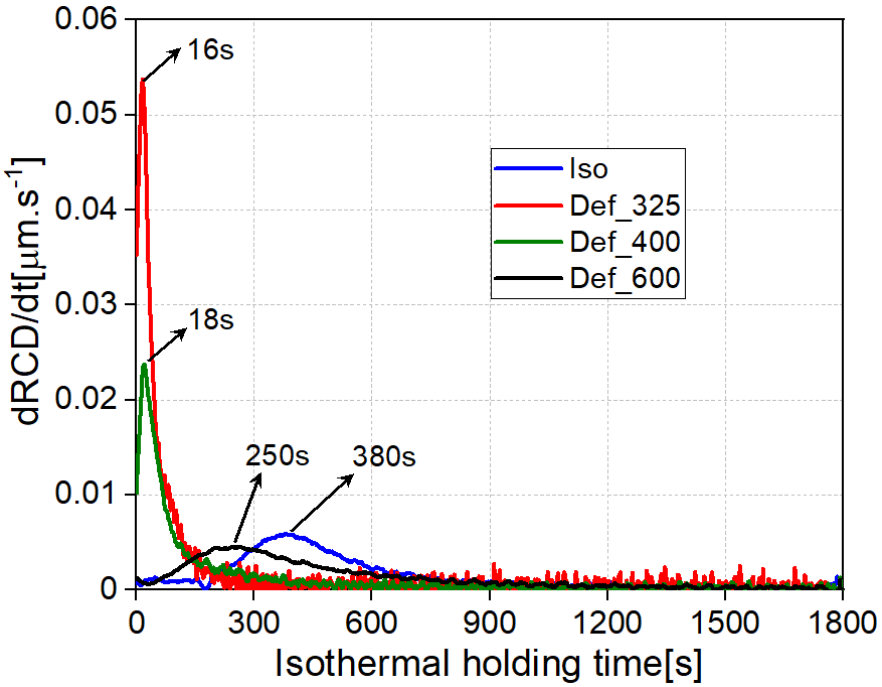

Figure 3 Transformation rate for pure isothermal and ausformed conditions: Iso is the non-ausformed condition, Def-600, Def-400, and Def_325 are ausforming at 600, 400, and 325 °C, respectively.

3.2 Microstructural analysis

The SEM micrographs in Figure 4 depict the changes occurring as a consequence of the applied deformation in longitudinal (L) and transverse (T) sections. Typically, regardless

of the test condition, the microstructures consisted of a bainitic matrix (α_b) with plate-like morphology with retained austenite in the form of blocks (RA_{block}) and film (RA_{film}), as illustrated in Figure 4a-L. Note that, considering the composition of the investigated steel, SEM examination of the microstructure did not reveal any presence of cementite particles.

As anticipated by the dilatometry results, both Iso and Def_600 microstructures in Figure 4a and 4b are comparable in both sections. It is clear then that deformation at 600 ^{o}C did not introduce relevant or detectable changes in the resulting microstructure compared to the pure isothermal specimen. The quantitative measurements reported in Table 2 show that the variation in the average bainite plate thickness ($t\alpha_b$) is the same in both L and T sections. Furthermore, the differences in $t\alpha_b$ between Iso and Def_600 conditions are within the measurement error margins. Eres-Castellanos et al. [1] and Hu et al. [9, 10] reported similar observations when the ausforming step was applied at a temperature above B_S in medium C -Si-rich alloyed steels.

The effect of the ausforming on the CFB microstructure is more noticeable at 400°C, as revealed by Figures 4c and 4d. The SEM images show a refinement of the microstructure and a very evident alignment of the bainitic ferrite plates with a specific angle to the deformation direction, as compared with the Iso and Def_600 conditions. The refinement of the microstructure being more pronounced with decreasing deformation temperature, as reported in Table 2.

Figure 5 shows the flow stress curves for the three deformation temperatures. The yield strength (σ_{ys}) of deformed austenite at 325 ^{o}C, using the 0.2% offset criterion, is about 695 MPa. This value drops to 600 and 450 MPa for Def_400 and Def_600 specimens, respectively. A comparison between the results of Table 2 and Figure 5 confirms that the higher is the strength of austenite, the thinner will be the bainitic ferrite plates; however, for an accurate analysis, the contribution from other factors, such as transformation kinetics and the carbon content of austenite, must also be taken into account [40]. Finally, as shown in Table 2, the average thickness of the bainite plates (166 nm) were measured for the sample isothermally treated at 325 ^{o}C without prior deformation (identified as 'Iso'). The thickness was reduced to about 100 nm when deformation was applied at 325 ^{o}C and then

the sample was held at the same temperature to allow for bainitic transformation; thereby, confirming the influence of applied stress on bainite plate thickness. It is well established that the strength of the parent austenite is one of the main parameters controlling the final scale of the bainitic ferrite plates. The shape change associated with the growth of bainite is elastically accommodated by the austenite, therefore, the higher the strength of austenite is, the higher the resistance to advance of the interface is, which it turns into smaller plates of bainite [41-43].

Table 2 Thickness of the bainite ferritic plate in the longitudinal ($t\alpha_b$–L) and transverse ($t\alpha_b$ –T) sections; and the average thickness ($t\alpha_b$) in nm.

Condition	**$t\alpha_b$–L (±8)**	**$t\alpha_b$–T (±7)**	**$t\alpha_b$**
Def_325	94	111	103
Def_400	140	125	133
Def_600	170	178	174
Iso	164	168	166

A systematic analysis of the bainitic ferrite growth angle to the deformation direction was performed to understand the observed alignment in the SEM micrographs. The alignment of the bainitic ferrite plate to a specific angle with respect to the deformation axis, Def_400, and Def_325 cases in Figure 4c and 4d were studied in further details. The statistical distribution of the alignment angle with respect to the deformation axis is reported in Figure 6. For comparison purposes, the same data with respect to the vertical axis was also measured for the non-ausformed specimen are shown in the same figure. It is worth noting that angle measurements were made only for the plates with an angle from zero to 90^o with respect to the deformation or vertical direction. In the pure isothermal (Iso) and Def_600 specimens, as illustrated in Figure 6a and 6b, the distribution was almost symmetrical within three main groups (10-19^o, 50-59^o, and 70-79^o) with slight differences in pure isothermal condition. This finding indicates that the growth of the bainite plates for pure isothermal and Def_600 is isotropic while it is anisotropic under the other investigated conditions.

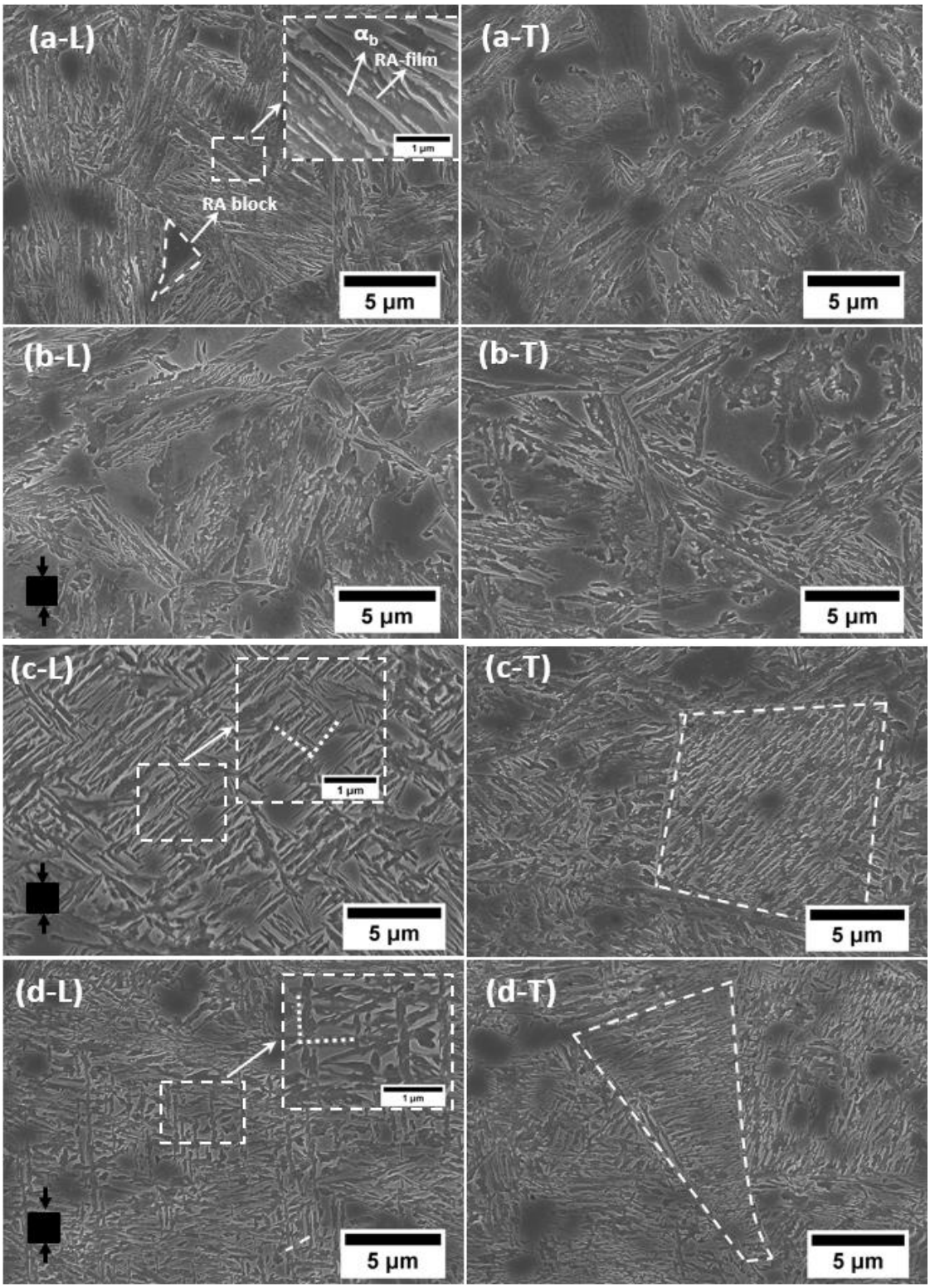

Figure 4 SEM micrographs for all experimental conditions, (a) pure isothermal, Iso; (b, c, and d) ausforming at 600 (Def_600), 400 (Def_400), and 325 ^{o}C (Def_325), respectively. L stands for the longitudinal section and T for the transverse section; RA-block, RA-film, and α_b are block-like, film-like retained austenite and bainitic ferrite, respectively.

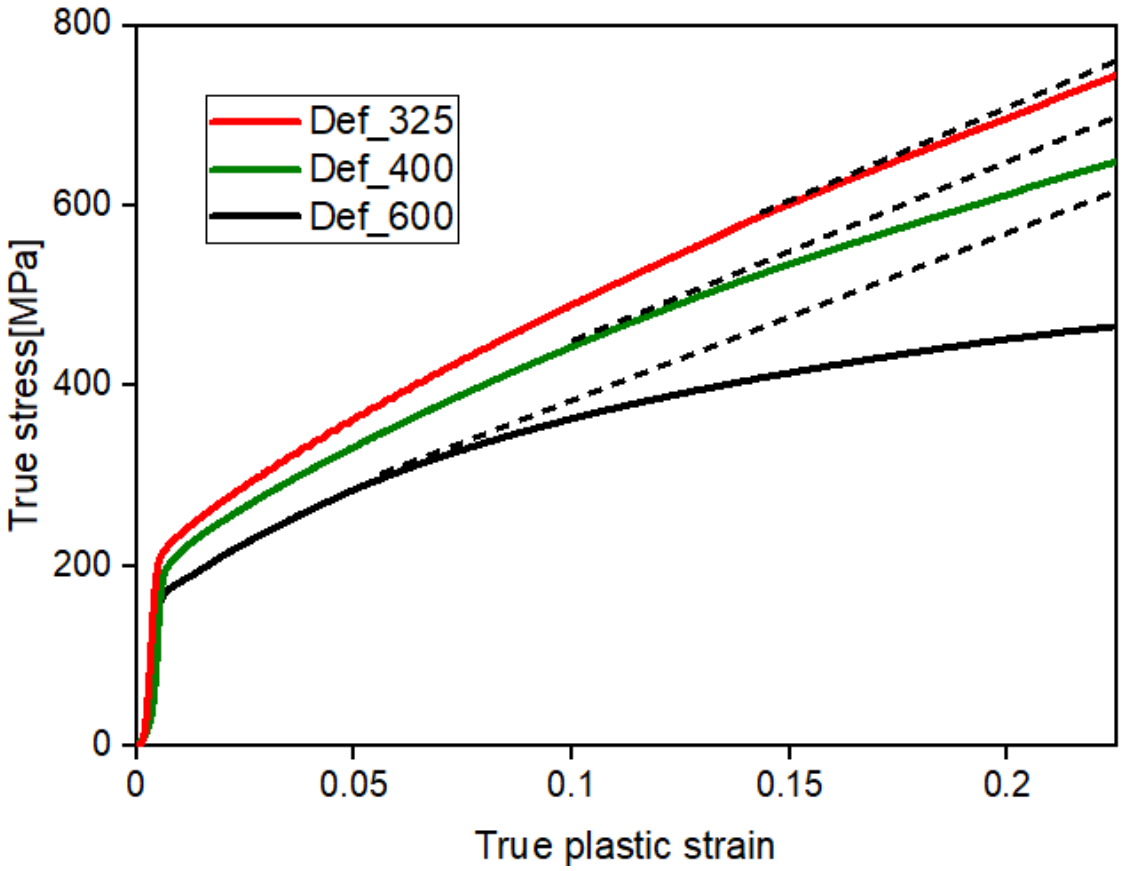

Figure 5 True stress vs. true plastic strain for ausforming conditions at 325, 400, and 600 ^{o}C. The dashed lines were plotted to illustrate the change in the slope of the curve with increased strain.

However, for low-temperature ausforming conditions (Def_400 and Def_325), the angle distribution was significantly different. In the Def_400 condition (Figure 4c-L), most of the bainite plates aligned with an angle of 40-60^{o} to the deformation direction axis with few plates having alignment angles < 10^{o} or >80^{o}, as shown in Figure 6c. The above findings are in good agreement with those of Eres-Castellanos et al. [1], who reported an alignment angle in the range of 45^{o} in medium CFB steel. While Zhou et al. [27] found that the angles were at an extent of 65-90^{o} when applied stress was below austenite yield strength during bainite transformation in medium C–Mn–Si alloy steel. In contrast, in the Def_325 specimen (Figure 4d-L), the bainitic ferrite plates were mostly aligned parallel (i.e., zero degree) or with an angle of about 80-90^{o} to the deformation direction; and only a few grains were aligned in the range of 40-60^{o} (Figure 6d). Such differences could be related to the variant selection in specific austenite grains, which promote the formation of bainite plates in particular directions when deforming at lower temperatures [1, 5, 10]. The

above findings suggest that a preferential growth with an alignment at a specific angle of the bainitic plates occurs when ausforming below the B_S temperature. This preferential alignment is probably the main reason for the observed contraction in the longitudinal direction (RCL) and the expansion (RCD) during bainitic transformation in Figure 2c and 2d [1, 44].

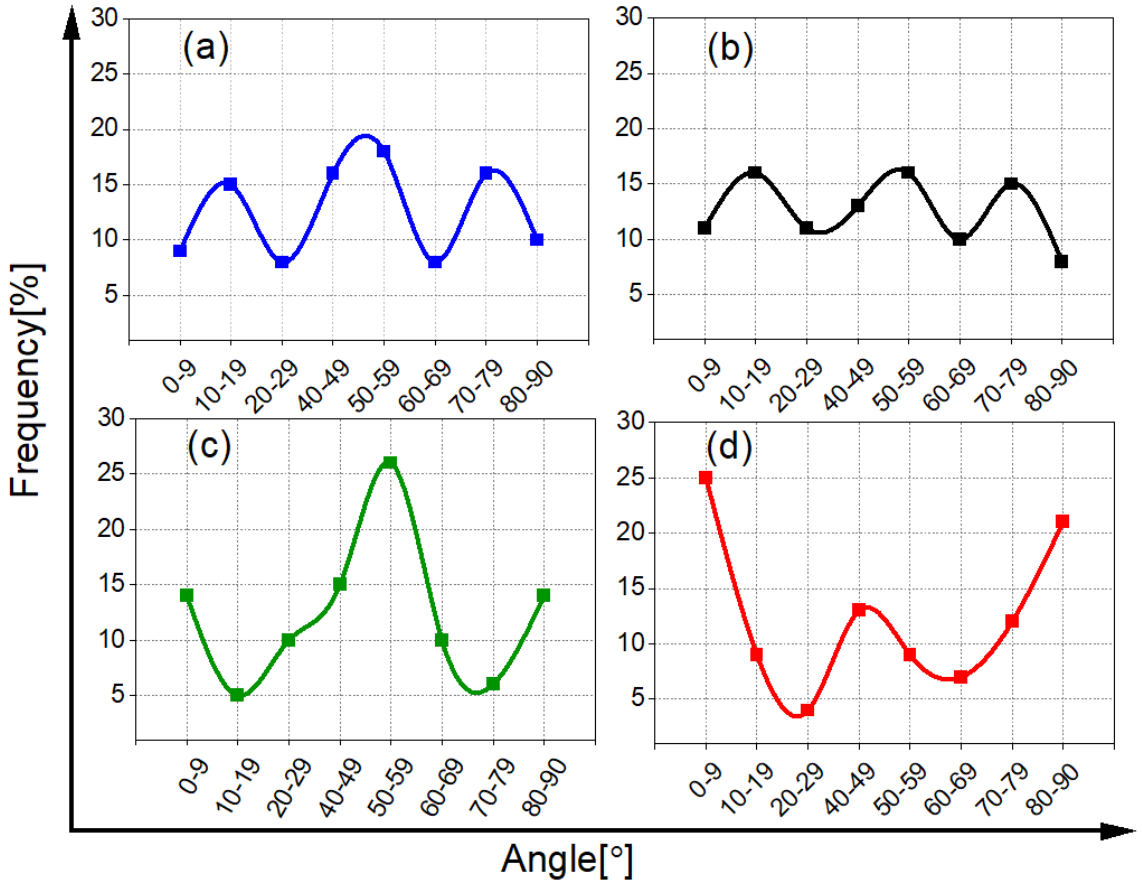

Figure 6 Angle distribution of bainitic ferrite plates in some austenite grains with the vertical axis as in (a) pure isothermal condition; or the deformation direction as in (b) Def_600, (c) Def_400, and (d) Def_325 conditions (the inserted images indicate the direction of bainite plate growth to the vertical axis).

3.3 Fractions of microstructural constituents

XRD investigation results, reported in Table 3, further confirm the microstructural characterization and dilatometric findings that ferrite (bainitic ferrite) and austenite, RA_T are the main phases present in the material. For instance, the results reported in Table 3 show that the amount of bainite (α_b) for Iso and Def_600 samples is almost identical, 0.86-

0.85, while it decreases as the ausforming temperature process decreases to 400 ºC and then to 325 °C. The above findings could be interpreted in terms of the increase in dislocation density. In fact, although plastic deformation increases the density of bainite nucleation sites, it also increases the dislocation density through the so-called mechanical stabilization phenomenon [45-51]. The generated dislocations hinder the movement of the glissile interfaces that must occur in order for the bainite plates to grow. As the ausforming temperatures decrease, more and more dislocations are created, and the austenite becomes stronger (see Figure 5), resulting in a significant slowdown of the bainitic transformation.

3.3.1 Evolution of the retained austenite

In order to determine the effect of ausforming on the RA, the EBSD phase maps of RA_{block} were analyzed for the different testing conditions, as shown in Figure 7. The results reveal that, with the pure isothermal case, Figure 7a, the size of the RA_{block} is reduced with decreasing ausforming temperature (Figure 7b-d). Further analysis could be made by comparing the ratio of blocky austenite regions to the total retained austenite, $\left[\frac{RA_{\cdot block}}{RA_T}\right]$, as reported in Table 3. The amount of blocky austenite decreases by almost 20% despite the increase in the fraction of retained austenite with decreasing temperature. This finding indicates that larger regions of untransformed austenite are partitioned (i.e., geometrically divided) by the formation of oriented bainitic ferrite plates during the Def_400 and Def_325 treatment. A desirable secondary effect of this blocky subdivision is that it enhances the presence of RA_{film}, which is thermally and mechanically more stable, improving the ductility and toughness response of the microstructure [52-54].

Hardness measurement results, also reported in Table 3, further confirm the positive impact of the refinement of both bainitic ferrite plates and retained austenite as well as austenite work hardening in increasing the hardness levels with decreasing ausforming temperatures.

Table 3 Volume fractions of the total retained austenite (RA_T) measured by XRD, blocky-shape (RA_{block}) estimated using EBSD and its corresponding percentage to the RA_T; and bainitic ferrite (α_b); hardness measurements. (note: all the measurement was done on the L section).

Condition	RA_T (±0.03)	RA_{block} (±0.03)	$\%\left[\frac{RA_{block}}{RA_T}\right]$	α_b (±0.03)	HV_{10} (±9)
Iso	0.13	0.11	84	0.87	435
Def_600	0.14	0.12	83	0.86	440
Def_400	0.21	0.15	68	0.79	490
Def_325	0.24	0.16	65	0.76	540

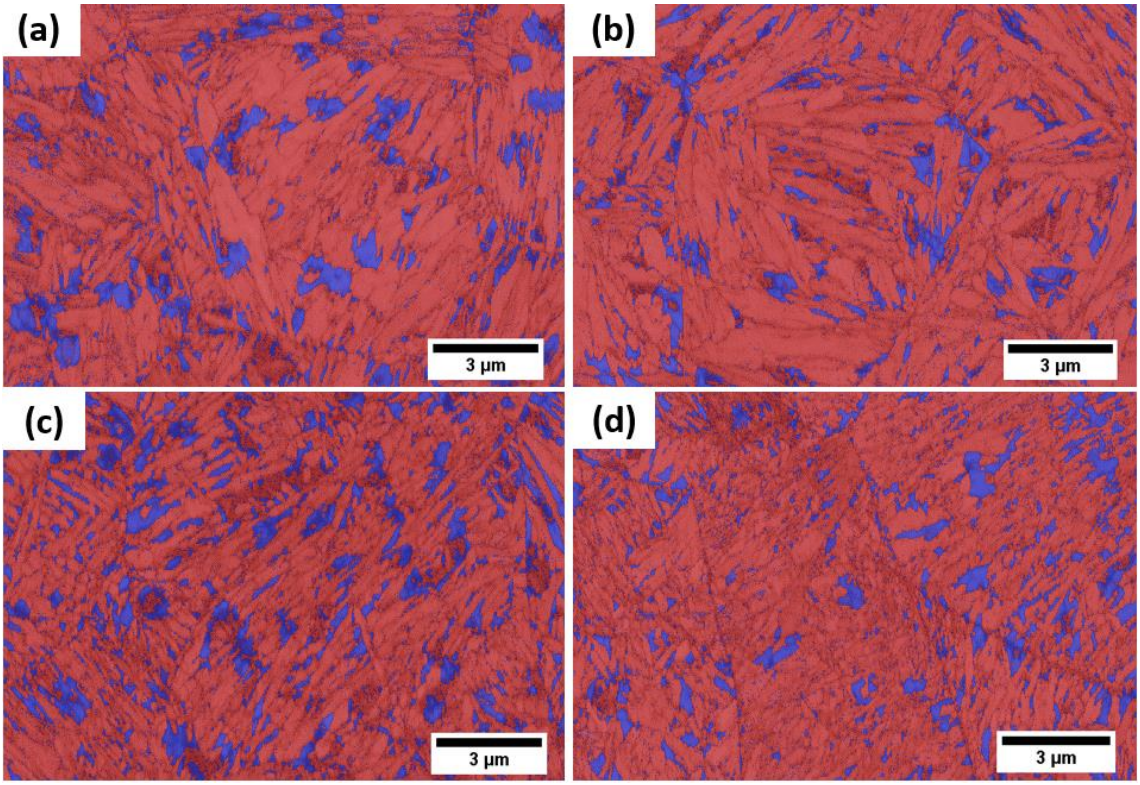

Figure 7 EBSD. phase map of RA_{block} for different conditions; (a) non-ausformed, (b) ausformed at 600 ºC, (c) ausformed at 400 ºC, and (d) ausformed at 325 ºC; blue and red are RA and bainitic ferrite phases, respectively. (Standard deviation is ±0.6%).

3.4 Evolution of RCV

It is generally accepted that a higher volume change, RCV, associated with bainitic transformation should be expected when more bainitic ferrite is formed. The RCV value intrinsically depends on the volume of the unit cell of the different phases and their corresponding fractions [5, 9, 27, 36, 55-57].

Such volume change can be calculated using the RCL and RCD signals in accordance with the approach proposed in the literature [58-60]:

$$RCV = \frac{\Delta V}{V_{iso}} = (1 + RCL)(1 + RCD)^2 - 1 \qquad \text{Equation 2}$$

Where ΔV is the volume change of the specimen, and V_{iso} is the volume of the specimen at the isothermal temperature.

However, as shown in Figure 8a, where RCV evolution is depicted for the different testing conditions, it is clear that the original premise, higher ferrite fraction leads to higher RCV value as in Def_325 sample, does not occur, where the XRD measurement in Figure 8b showed that the fraction of bainite for Def_325 sample was the lowest. Therefore, another factor must be considered to explain the observed behavior as described in the next section.

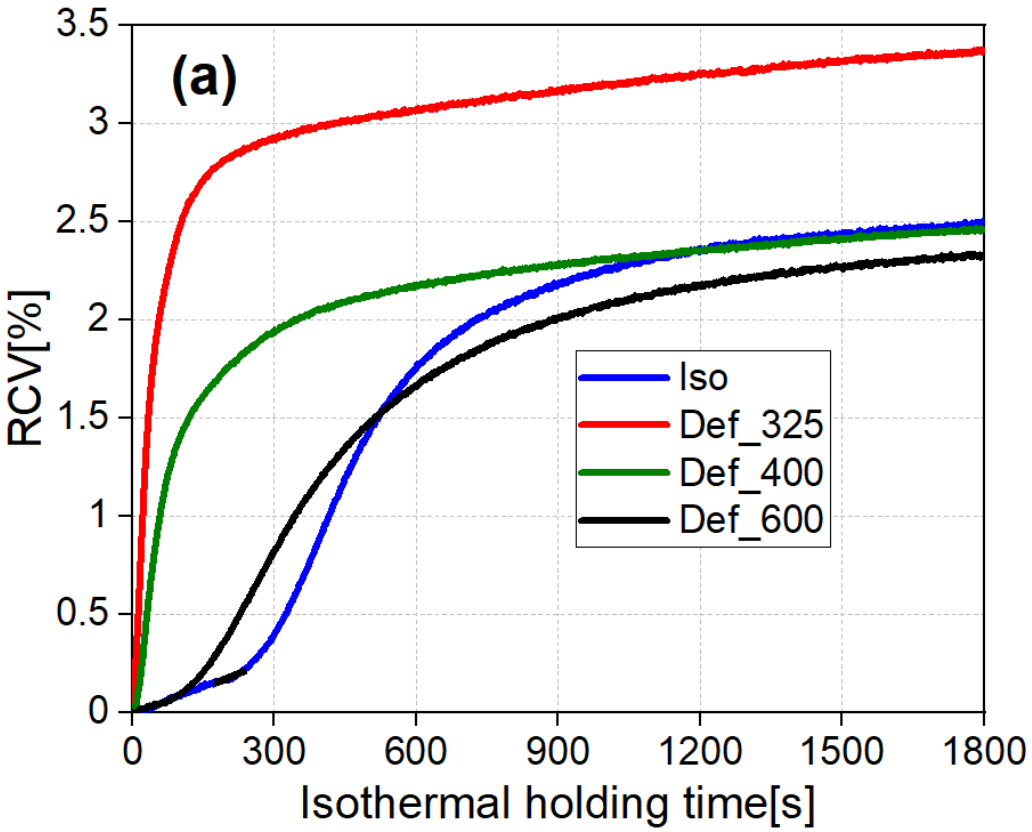

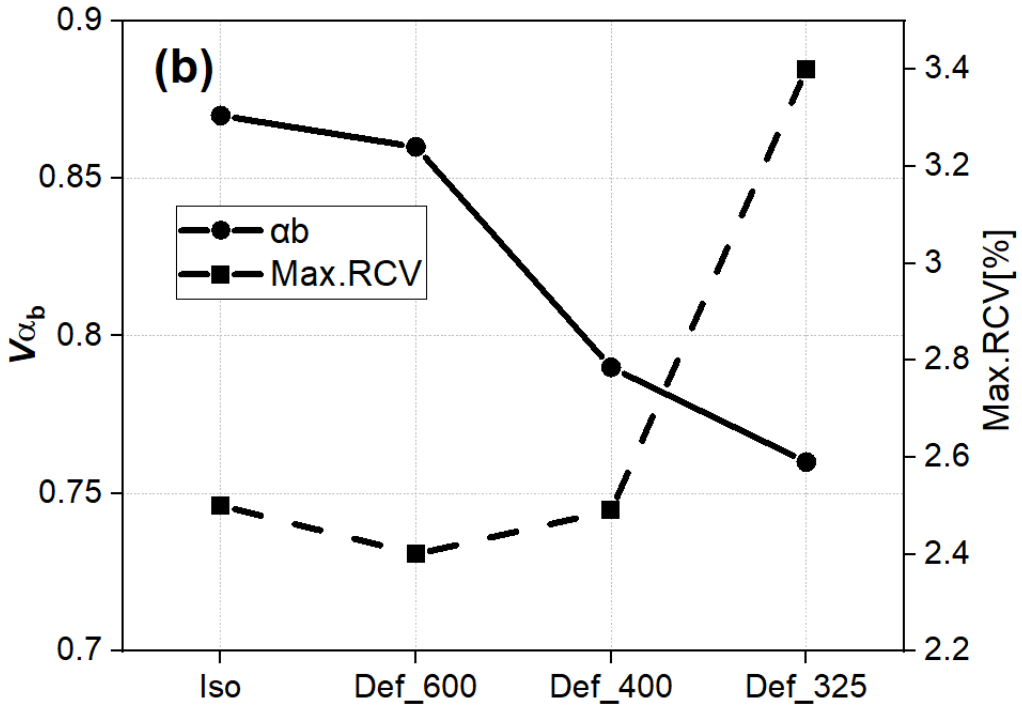

Figure 8 (a) RCV for all tested conditions; (b) volume fraction of α_b vs. the maximum RCV values.

3.5 Evolution of transformation plasticity strains (TP)

As described in the introduction of this manuscript, there is still another important factor that must be considered before a proper interpretation of the RCV curves is done, i.e., transformation plasticity associated with the bainitic transformation.

The development of the TP strains is related to the changes in volume strain during any displacive transformation, such as bainite, and it can be calculated according to the following expression [13, 25, 27]:

$$\overline{TP} = \frac{1}{2}(RCL - 2RCD + 0.33RCV) \qquad \text{Equation 1}$$

where $\overline{TP}$ is the mean values of the transformation plasticity strains in the longitudinal and transverse directions.

The evolution of TP strain as a function of the ausforming temperature is illustrated in Figure 9a. The increment of the TP strains reaches a steady-state toward the end of the isothermal transformation holding time. This indicates that TP strains decrease as the bainite transformation diminishes. This finding agrees with those reported by Liu [14], who also reported a reduction of the TP strains with the holding time in a medium carbon CFB steel.

TP strains could be divided into two categories according to their intensities: the first group, Iso, and Def_600 conditions, the TP strains were minimal indicating that the TP strains in the longitudinal and transverse directions nearly cancel out each other. Although the TP curve for specimen deformed at 600 ^{o}C, started to deviate slightly at about 100 s towards the negative sign, it eventually reverts to zero. The slight increase in TP strain could be related to the preferably oriented bainite plates in some austenite grains due to the deformation, which reduces the deformation effect and allows other variants to grow randomly, such that in the no-deformed condition. The obtained results are in good agreement with the growth distribution angle of bainite plates reported in Figure 6 and the dilatation in Figure 2. Bhadeshia et al. and Matsuzaki et al. [13, 58] found that when higher stresses are applied during bainite transformation in low carbon steel, the negative transverse strain evolved towards the positive sign as the transformation progressed further. The authors inferred that some variants grow favourably with the stress and others do not. When the number of variants that align or favorably grow in the direction of the applied stress is small, then the microstructure is called isotropic in regard to the variants.

In the second group, Def_400 and Def_325 conditions, the TP strains were more significant and deviated from zero toward higher negative values (see Figure 9). The TP strain developed in the Def_325 specimen was slightly higher than the one in the Def_400 specimen. Furthermore, as reported in Figure 6d, many bainitic plates were aligned at an angle of 0 or 90 degrees with the deformation axis. This behaviour could be explained in terms of a strong variant selection that occurred for some bainite plates in specific austenite grains when the ausforming took place at lower temperatures and supports the arguments in favour of the effect of deformation on variant selection during the growth of bainitic plates. [39, 61, 62]. Thus, variant selection could be another factor contributing to higher

radial dilatation signal at the expense of axial dilatation, as demonstrated in the results reported in Figure 2.

Furthermore, the TP strains in the Def_325 specimen started to increase at around 600 s and became closer to the TP strain in the Def_400 specimen at the end of the isothermal holding. This can be attributed to the larger driving force for transformation gained under these conditions that overcome the anisotropic growth in bainite plates when the ausforming process is applied at lower temperatures before bainite transformation [1].

The relationship between the volume fraction of transformed bainite and the highest value of the TP strain is represented in Figure 9b. The TP strain response to the progress of the bainite transformation is changing according to the ausforming states, i.e., first or second group. The TP amplified remarkably during the bainite transformation following ausforming below B_S (second group), while in the first group (Iso and Def_600), the increase in TP strain was nearly constant (almost zero) regardless of the amount of transformed bainite.

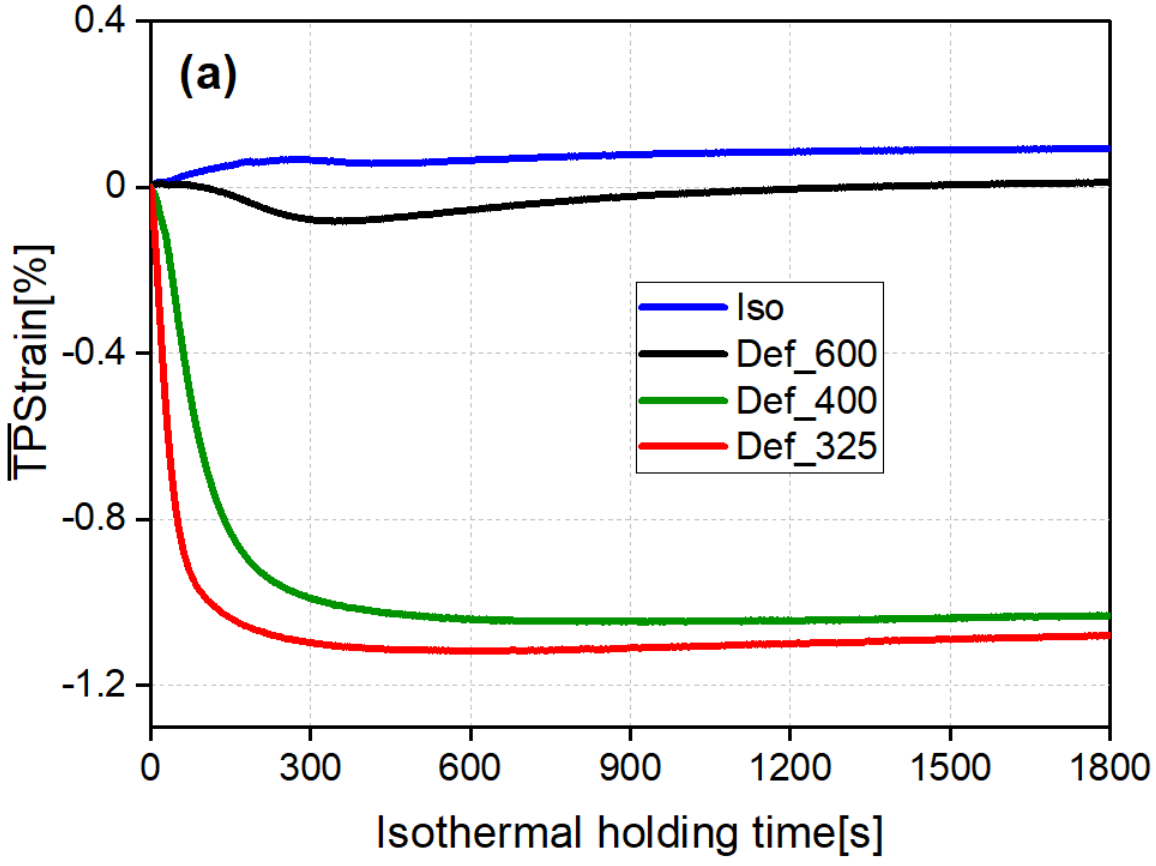

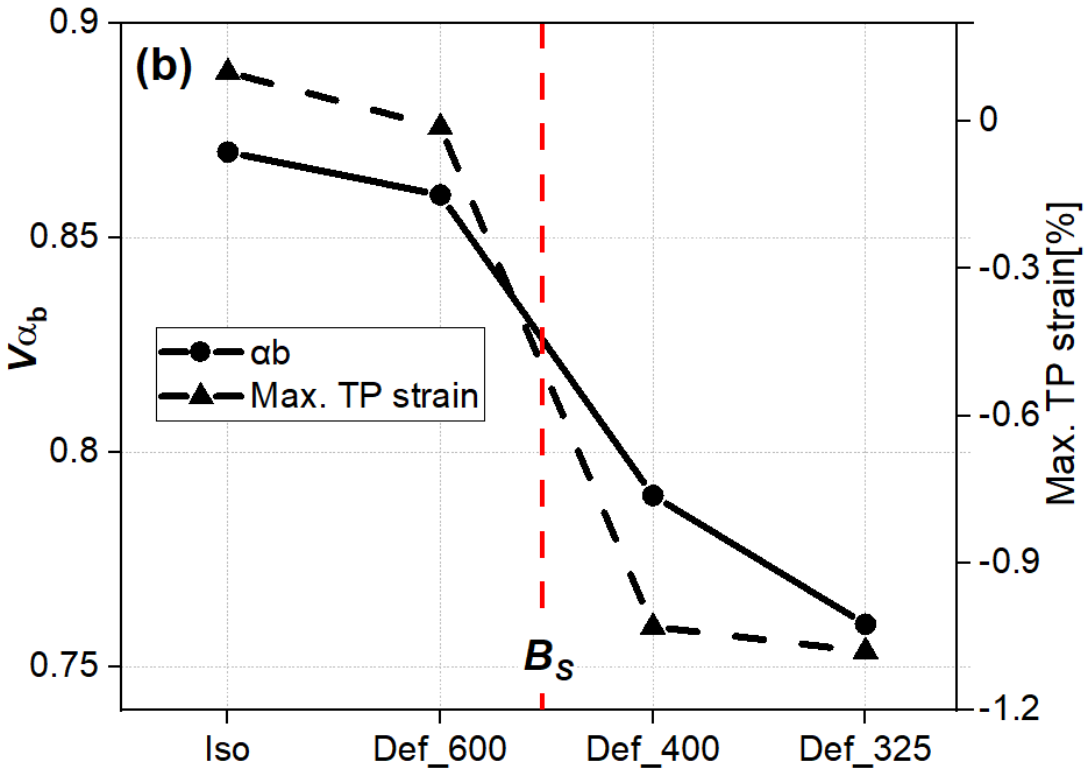

Figure 9 (a) evolution of TP strains during bainite transformation holding time; (b) volume fraction of α_b vs. and the maximum TP strain in all tested conditions. The dashed red line shows an imaginary limit between ausforming above and below the B_S temperature.

In order to confirm the above results, the orientation of bainite was analyzed by the EBSD technique. The maps were taken at low magnifications to cover a large area (about 1600 μm^2) with a step size of 100 nm. The total number of pixels was 120000 and the confidential index (CI) value was taken to be 9 for all conditions (Figure 10). The loading direction is shown in each image. In this figure, the elongated colored shape represents a bainitic block that aggregates of subunits (or plates) of ferrite of the same variant or two variants misoriented by a small angle (<15^o) [63]. The morphology and number of variants did not differ much between the pure isothermal specimen and the high temperature (600 ^{o}C) ausformed one, where many variants were formed and randomly aligned in one austenite grain (i.e., black dashed lines in Figure 10). Moreover, the variations in the orientation map with respect to the (001) direction between the longitudinal section (Figure 10a-T and 10b-T) are minor for both conditions.

The results also agree well with the evolution of the TP strain, as reported in Figure 9. However, for the lower ausforming temperature conditions, there were few preferably oriented variants formed in each deformed austenite, as can be seen in Figure 10d-L and 10d-T. The above results are in agreement with those reported by Liu and Lambers, who also found that the number of bainitic ferrite variants decreased with compressive elastic and plastic stresses applied during bainite transformation and resulted in a strong variant selection [14, 15]. Furthermore, Figure 10c-L and 10d-L show that the variant orientation within the L sections is entirely different from the one in the T sections (Figure 10c-T and 10d-T). This difference could be linked to the presence of a strong texture under these conditions. The above findings are also consistent with the results reported in Figure 6, where it can be seen that the bainite plates in Iso and Def_600 specimens are distributed almost uniformly at three different angles around the vertical axis. In contrast, in the Def_400 and Def_325 specimens, the distribution of the angles was non-symmetrical. The influence of plastic deformation and superimposed stress on bainitic transformation was also reported by Liu et al. [14] and Lambers et al. [23]], who found that limited bainite variants formed in the austenite and were aligned at a specific direction when a plastic deformation was applied prior to the bainite transformation.

Figure 11a-d illustrate the Pole Figures (PF) for the investigated conditions. The transformation texture takes place when some variants show higher pole figure intensity, indicating their prevalence over others. Therefore, when the strong variant selection exist, texture with strong peaks develops in the sample. This can be illustrated in PF with colour legend. Red means strong texture and blue is weak texture. The crystallographic variants deceased significantly in low temperature ausforming conditions (400 and 325 ^{o}C), as seen in Figure 11c and 11, compared to the pure isothermal and ausforming at 600 ^{o}C conditions (Figure 11a-11b). Furthermore, the PFs showed that texture evolution of bainitic ferrite a clear deformation texture in the case of Def_400 and Def_325 samples compared to a weaker one in the case of Iso and Def_600 sample.

Figure 11e shows the relationship between the texture intensity and the ausforming state. It can be seen that the T section always has the highest level of texture regardless of testing condition. Moreover, Interestingly, the texture level in the specimen ausformed at 400 ^{o}C,

especially in the L section, is higher than the one in the specimen deformed at 325 ^{o}C for the same section. This behavior was also seen in the TP strains evolution, as reported in Figure 9. This could be related to the higher amount of bainite transformed when the deformation takes place at the transformation temperature [1]. The lower transformation rate can also explain the decrease in texture intensity in specimens ausformed at 600 ^{o}C compared with the pure isothermal specimen.

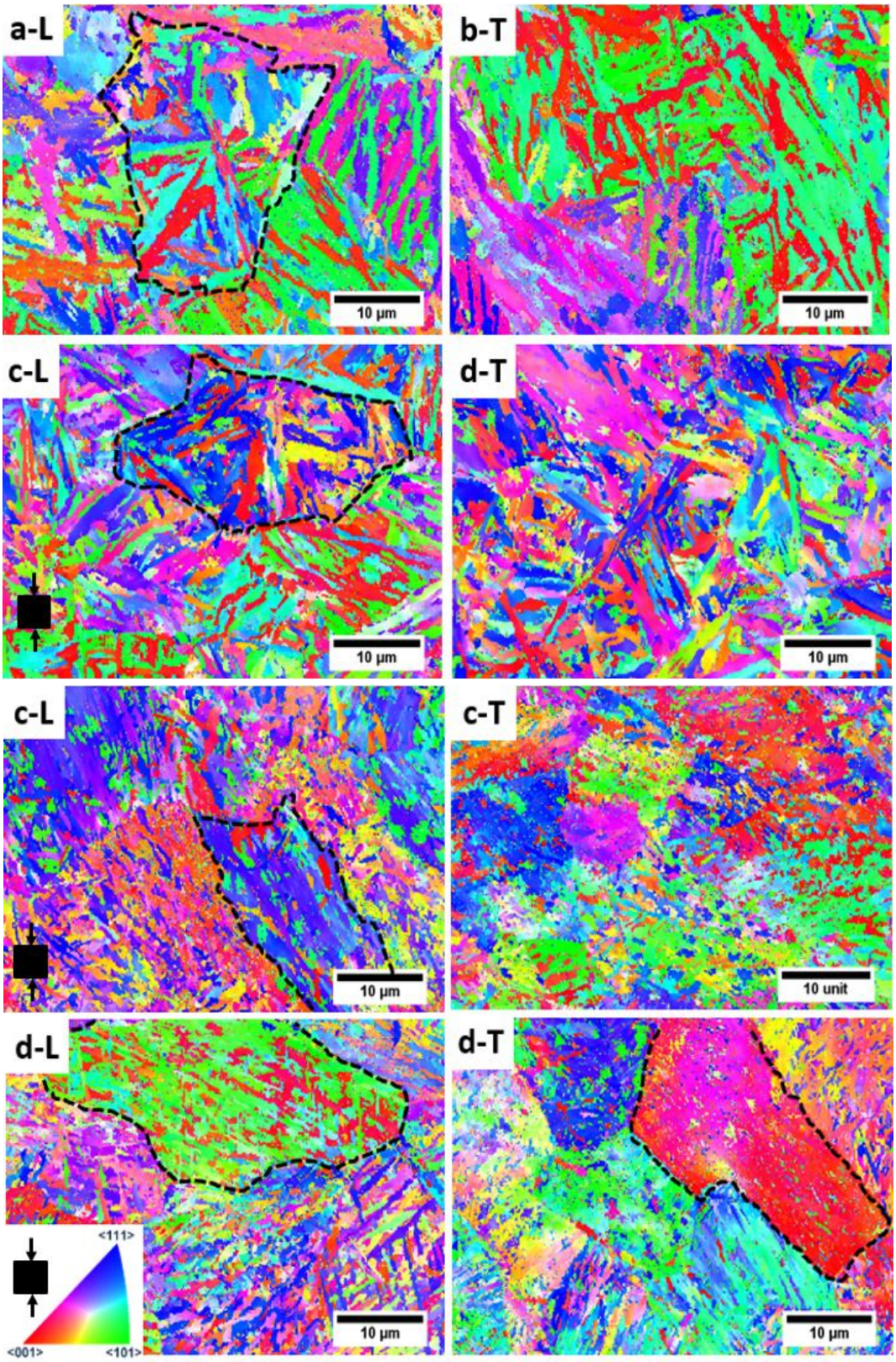

Figure 10 Orientation imaging maps in (001) α_b direction in the specimens with different conditions: (a) non-ausformed; (b) ausformed at 600 °C; (c) ausformed at 400 °C; (d) ausformed at 325 °C, L and T are longitudinal and transverse respectively (black dashed lines are PAGB).

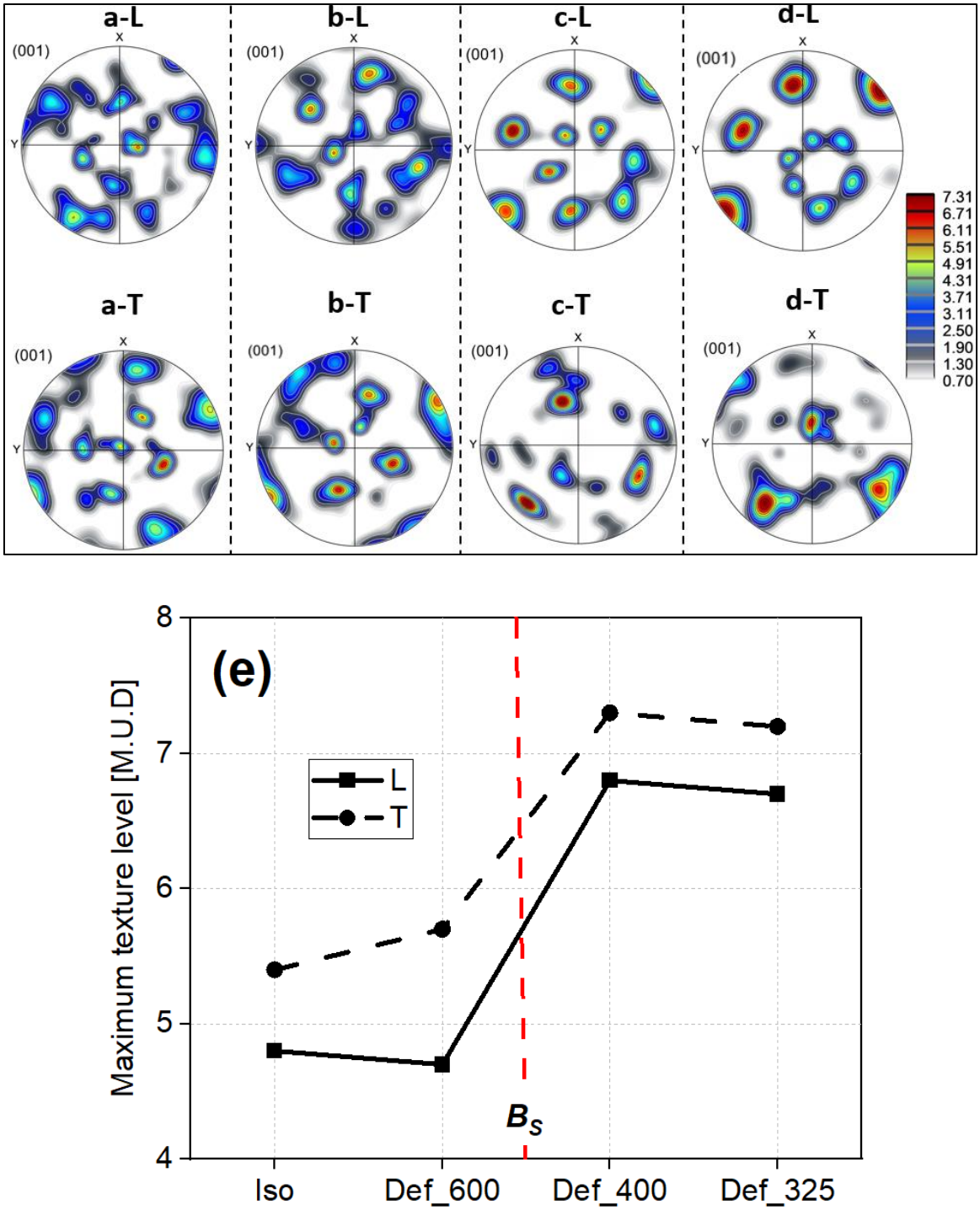

Figure 11 PFs of bainitic ferrite phase treated with different conditions: (a) non-ausformed; (b) ausformed at 600 °C; (c) ausformed at 400 °C; (d) ausformed at 325 °C, L and T are longitudinal and transverse respectively; (e) the difference in texture level of all conditions for longitudinal (L) and transverse (T) sections. The dashed red line shows an imaginary limit between ausforming above and below the B_S temperature.

Conclusion

The influence of different ausforming temperatures in altering the morphology of a CFB microstructure and its relationship to the transformation plasticity strains (TP) was studied in a medium carbon- high Si steel. The findings can be summarized as follows:

1. The effect of ausforming above B_S temperature was negligible on the bainitic ferrite plate thickness and its morphology, compared to pure isothermal condition.
2. Low-temperature ausforming (325 or 400 ^{o}C) prior to bainite transformation leads to an anisotropic microstructure accompanied by a remarkable refinement of the bainitic ferrite plates to reach a nanoscale level (~100 nm).
3. Volume strain cannot be considered an indication of austenite's boost to bainite transformation when the deformation occurred below B_S temperature.
4. Bainite plates were aligned randomly in the case of pure isothermal and ausforming at 600 °C. In comparison, an alignment at a specific angle, 45^{o,} and 0-90^{o} was the characteristic of the specimen ausformed at 400 and 325 ^{o}C, respectively.
5. TP strains were amplified during bainitic transformation when the ausforming was below B_S (400 and 325 ^{o}C) and resulted from the alignment and strong texturing of CFB microstructure.

Acknowledgment

This research is part of a Ph.D. scholarship awarded by the Ministry of Higher Education and Scientific Research in Libya in cooperation with the Canadian Office for International Education (CBIE).

Data availability

The raw/processed data required to reproduce these findings cannot be shared at this time as the data also forms part of an ongoing study.

References

[1] A. Eres-Castellanos, L. Morales-Rivas, A. Latz, F. G. Caballero, and C. Garcia-Mateo, "Effect of ausforming on the anisotropy of low temperature bainitic transformation," *Materials Characterization,* vol. 145, pp. 371-380, 2018, doi: 10.1016/j.matchar.2018.08.062.

[2] J. Zhao *et al.*, "Transformation behavior and microstructure feature of large strain ausformed low-temperature bainite in a medium C - Si rich alloy steel," *Materials Science and Engineering: A,* vol. 682, pp. 527-534, 2017, doi: 10.1016/j.msea.2016.11.073.

[3] H. Hu, G. Xu, L. Wang, and M. Zhou, "Effects of Strain and Deformation Temperature on Bainitic Transformation in a Fe-C-Mn-Si Alloy," *steel research international,* vol. 88, no. 3, 2017, doi: 10.1002/srin.201600170.

[4] H.-l. Fan, A.-m. Zhao, Q.-c. Li, H. Guo, and J.-g. He, "Effects of ausforming strain on bainite transformation in nanostructured bainite steel," *International Journal of Minerals, Metallurgy, and Materials,* journal article vol. 24, no. 3, pp. 264-270, 2017, doi: 10.1007/s12613-017-1404-7.

[5] L. Zhao *et al.*, "The combining effects of ausforming and below-Ms or above-Ms austempering on the transformation kinetics, microstructure and mechanical properties of low-carbon bainitic steel," *Materials & Design,* vol. 183, 2019, doi: 10.1016/j.matdes.2019.108123.

[6] M. Zhang, Y. H. Wang, C. L. Zheng, F. C. Zhang, and T. S. Wang, "Effects of ausforming on isothermal bainite transformation behaviour and microstructural refinement in medium-carbon Si–Al-rich alloy steel," *Materials & Design* vol. 62, pp. 168-174, 2014, doi: 10.1016/j.matdes.2014.05.024.

[7] M. Zhang, T. S. Wang, Y. H. Wang, J. Yang, and F. C. Zhang, "Preparation of nanostructured bainite in medium-carbon alloy steel," *Materials Science and Engineering: A,* vol. 568, pp. 123-126, 2013, doi: 10.1016/j.msea.2013.01.046.

[8] B. B. He, W. Xu, and M. X. Huang, "Effect of ausforming temperature and strain on the bainitic transformation kinetics of a low carbon boron steel," *Philosophical Magazine,* vol. 95, no. 11, pp. 1150-1163, 2015, doi: 10.1080/14786435.2015.1025886.

[9] H. Hu, G. Xu, F. Dai, J. Tian, and G. Chen, "Critical ausforming temperature to promote isothermal bainitic transformation in prior-deformed austenite," *Materials Science and Technology,* vol. 35, no. 4, pp. 420-428, 2019, doi: 10.1080/02670836.2019.1567663.

[10] H.-j. Hu, H. S. Zurob, G. Xu, D. Embury, and G. R. Purdy, "New insights to the effects of ausforming on the bainitic transformation," *Materials Science and Engineering: A,* vol. 626, pp. 34-40, 2015, doi: 10.1016/j.msea.2014.12.043.

[11] Garcia-Mateo and F. G. Caballero, "Advanced High Strength Bainitic Steels," pp. 165-190, 2014, doi: 10.1016/b978-0-08-096532-1.00114-x.

[12] H. K. D. H. Bhadeshia, "Bainite-in-Steels," *Materials Science & Metallurgy,* 2002.

[13] H. K. D. H. Bhadeshia, S. A. David, J. M. Vitek, and R. W. Reed, "Stress induced transformation to bainite in Fe–Cr–Mo–C pressure vessel steel," *Materials Science and Technology,* vol. 7, no. 8, pp. 686-698, 2013, doi: 10.1179/mst.1991.7.8.686.

[14] M. Liu, Y. Ma, G. Xu, G. Cai, M. Zhou, and X. Zhang, "Effects of Plastic Stress on Transformation Plasticity and Microstructure of a Carbide-Free Bainite Steel," *Metallography, Microstructure, and Analysis,* journal article vol. 8, no. 2, pp. 159-166, 2019, doi: 10.1007/s13632-019-00527-2.

[15] S. T. H.-G. Lambers, H.J. Maier, D. Canadinc, "Evolution of transformation plasticity during bainitic transformation," *Metallurgical and Materials Transactions A,* vol. 102, pp. 1152-1163, 2011.

[16] H. N. Han and D.-W. Suh, "A model for transformation plasticity during bainite transformation of steel under external stress," *Acta Materialia,* vol. 51, no. 16, pp. 4907-4917, 2003, doi: 10.1016/s1359-6454(03)00333-1.

[17] L. Morales-Rivas *et al.*, "Crystallographic examination of the interaction between texture evolution, mechanically induced martensitic transformation and twinning in nanostructured bainite," *Journal of Alloys and Compounds,* vol. 752, pp. 505-519, 2018, doi: 10.1016/j.jallcom.2018.04.189.

[18] X. L. W. B.B. Wu, Z.Q. Wang, J.X. Zhao, Y. H. Jin, C.S. Wang, C.J. Shang, R.D.K. Misra, R. D. K., "New insights from crystallography into the effect of refining prior austenite grain size on transformation phenomenon and consequent mechanical properties of ultra-high strength low alloy steel," 2018.

[19] S. Grostabussiat, L. Taleb, J. F. Jullien, and F. Sidoroff, "Transformation induced plasticity in martensitic transformation of ferrous alloys," *J Phys Iv,* vol. 11, no. PR4, pp. Pr4-173-Pr4-180, 2001, doi: 10.1051/jp4:2001422.

[20] C. L. Magee, H. W. Paxton, and C. I. O. T. P. PA., *Transformation Kinetics, Microplasticity and Aging of Martensite in Fe-31Ni*. Carnegie Inst. of Technology, 1966.

[21] G. W. Greenwood, R. H. Johnson, and L. Rotherham, "The deformation of metals under small stresses during phase transformations," *Proceedings of the Royal Society of London. Series A. Mathematical and Physical Sciences,* vol. 283, no. 1394, pp. 403-422, 1997, doi: 10.1098/rspa.1965.0029.

[22] M. Zhou, G. Xu, H. Hu, Q. Yuan, and J. Tian, "Kinetics model of bainitic transformation with stress," *Metals and Materials International,* vol. 24, no. 1, pp. 28-34, 2018, doi: 10.1007/s12540-017-7261-0.

[23] H. G. Lambers, D. Canadinc, and H. J. Maier, "Evolution of transformation plasticity in austenite-to-bainite phase transformation: A multi parameter problem," *Materials Science and Engineering: A,* vol. 541, pp. 73-80, 2012, doi: 10.1016/j.msea.2012.02.004.

[24] Z. Liu, K. F. Yao, and Z. Liu, "Quantitative research on effects of stresses and strains on bainitic transformation kinetics and transformation plasticity," *Materials Science and Technology,* vol. 16, no. 6, pp. 643-647, 2013, doi: 10.1179/026708300101508216.

[25] G. I. Rees and P. H. Shipway, "Modelling transformation plasticity during the growth of bainite under stress," *Materials Science and Engineering: A,* vol. 223, no. 1-2, pp. 168-178, 1997, doi: 10.1016/s0921-5093(96)10478-0.

[26] M. C. Uslu, D. Canadinc, H. G. Lambers, S. Tschumak, and H. J. Maier, "Modeling the role of external stresses on the austenite-to-bainite phase transformation in 51CrV4 steel," *Modelling and Simulation in Materials Science and Engineering,* vol. 19, no. 4, p. 045007, 2011, doi: 10.1088/0965-0393/19/4/045007.

[27] M. Zhou, G. Xu, L. Wang, and Q. Yuan, "The Varying Effects of Uniaxial Compressive Stress on the Bainitic Transformation under Different Austenitization Temperatures," *Metals-Basel,* vol. 6, no. 5, 2016, doi: 10.3390/met6050119.

[28] S. T. H.-G. Lambers, H.J. Maier, D. Canadinc, "Pre-deformation–transformation plasticity relationship during martensitic transformation," *Materials Science and Engineering* vol. A 527, pp. 625–633, 2010.

[29] M. J. S. Francisca García CABALLERO, Carlos CAPDEVILA, Carlos GARCÍA-MATEO and Carlos GARCÍA DE ANDRÉS, "Design of Advanced Bainitic Steels by Optimisation of TTT Diagrams and T0 Curves," *Isij Int,* vol. 46, 2006.

[30] H. K. D. H. Bhadeshia, "NEW BAINITIC STEELS BY DESIGN," *The Minerals, Metals and Materials Society,* 1989.

[31] M. Zorgani, C. Garcia-Mateo, and M. Jahazi, "The role of ausforming in the stability of retained austenite in a medium-C carbide-free bainitic steel," *Journal of Materials Research and Technology,* vol. 9, no. 4, pp. 7762-7776, 2020, doi: 10.1016/j.jmrt.2020.05.062.

[32] H. K. D. H. B. S. Singh, "Estimation of bainite plate-thickness in low-alloy steels," *Materials Science and Engineering: A,* vol. 245, no. 1, pp. 72-79, 1998, doi: 10.1016/s0921-5093(97)00701-6.

[33] J.-J. F. B. Beausir, "Analysis Tools for Electron and X-ray diffraction, ATEX - software," *Université de Lorraine Metz,* 2017. [Online]. Available: http://www.atex-software.eu/.

[34] C. F. Jatczak, "Retained Austenite and Its Measurement by X-Ray Diffraction," *SAE Transactions,* vol. 89, pp. 1657-1676, 1980.

[35] A. E975-13, "Standard Practice for X-Ray Determination of Retained Austenite in Steel with Near Random Crystallographic Orientation," *ASTM International, West Conshohocken, PA,* 2013, doi: 10.1520/e0975-13.

[36] G. X. Ming-xing Zhou, Li Wang, Zheng-Liang Xue, and Hai-Jiang Hu, "Comprehensive Analysis of the Dilatation During Bainitic Transformation Under Stress," 2015.

[37] G. Mingxing Zhou, Yulong Zhang, Zhengliang Xue, "The effects of external compressive stress on the kinetic of flow temperature bainitic transformation and microstructure in a superbainite steel," *International Journal of Materials Research,* 2015.

[38] P. H. Shipway and H. K. D. H. Bhadeshia, "Mechanical stabilisation of bainite," *Materials Science and Technology,* vol. 11, no. 11, pp. 1116-1128, 2013, doi: 10.1179/mst.1995.11.11.1116.

[39] W. Gong, Y. Tomota, Y. Adachi, A. M. Paradowska, J. F. Kelleher, and S. Y. Zhang, "Effects of ausforming temperature on bainite transformation, microstructure and variant selection in nanobainite steel," *Acta Materialia,* vol. 61, no. 11, pp. 4142-4154, 2013, doi: 10.1016/j.actamat.2013.03.041.

[40] A. Eres-Castellanos *et al.*, "Assessing the scale contributing factors of three carbide-free bainitic steels: A complementary theoretical and experimental approach," *Materials & Design,* vol. 197, p. 109217, 2021, doi: 10.1016/j.matdes.2020.109217.

[41] S. B. Singh and H. K. D. H. Bhadeshia, "Estimation of bainite plate-thickness in low-alloy steels," *Materials Science and Engineering: A,* vol. 245, no. 1, pp. 72-79, 1998/04/30/ 1998, doi: https://doi.org/10.1016/S0921-5093(97)00701-6.

[42] J. Cornide, C. Garcia-Mateo, C. Capdevila, and F. G. Caballero, "An assessment of the contributing factors to the nanoscale structural refinement of advanced bainitic steels," *Journal of Alloys and Compounds,* vol. 577, no. Suppl1, pp. S43-S47, 2013, doi: DOI:101016/jjallcom201111066.

[43] Z. Yang *et al.*, "Accelerating nano-bainite transformation based on a new constructed microstructural predicting model," *Materials Science and Engineering: A,* vol. 748, pp. 16-20, 2019/03/04/ 2019, doi: https://doi.org/10.1016/j.msea.2019.01.061.

[44] C. E.-C. García Mateo, A.; García Caballero, Francisca; Lazt, Andreas; Schreiber, Sebastian; Ray, Arunim; Bracke, Lieven; Somani, Mahesh; Kaikkonen, Pentti; Pohjonen, Aarne; Porter, David A., "Towards industrial applicability of (medium C) nanostructured bainitic steels (TIANOBAIN)," 2020.

[45] D. S. Schicchi and M. Hunkel, "Transformation plasticity and kinetic during bainite transformation on a 22MnB5 steel grade," *Materialwissenschaft und Werkstofftechnik,* vol. 47, no. 8, pp. 771-779, 2016, doi: 10.1002/mawe.201600611.

[46] J. Min, L. G. Hector, L. Zhang, J. Lin, J. E. Carsley, and L. Sun, "Elevated-temperature mechanical stability and transformation behavior of retained austenite in a quenching

and partitioning steel," *Materials Science and Engineering: A,* vol. 673, pp. 423-429, 2016, doi: 10.1016/j.msea.2016.07.090.

[47] A. Z. C. Zhi, J. He & H. Yang, "Effect of multi-step ausforming process on the microstructure evaluation of nanobainite steel," 2016.

[48] H.-S. W. S. Chatterjee, J. R. Yang and H. K. D. H. Bhadeshia, "Mechanical stabilisation of austenite," *Mater. Sci. Technol,* vol. 22, pp. 641–644, 2006.

[49] C. Y. H. J.R.Yang, W.H. Hsieh, and C.S. Chiou, "Mechanicla stablization of austenite against Bainitic reaction in Fe-Mn-Si-C Bainitic steel," *Mater. Trans. ,* vol. JIM 37 pp. 579–585, 1996.

[50] K. Tsuzaki, S.-i. Fukasaku, Y. Tomota, and T. Maki, "Effect of Prior Deformation of Austenite on the γ→ε Martensitic Transformation in Fe–Mn Alloys," *Materials Transactions, JIM,* vol. 32, no. 3, pp. 222-228, 1991, doi: 10.2320/matertrans1989.32.222.

[51] M. Maalekian, E. Kozeschnik, S. Chatterjee, and H. K. D. H. Bhadeshia, "Mechanical stabilisation of eutectoid steel," *Materials Science and Technology,* vol. 23, no. 5, pp. 610-612, 2013, doi: 10.1179/174328407x158686.

[52] G. Chen, H. Hu, G. Xu, J. Tian, X. Wan, and X. Wang, "Optimizing Microstructure and Property by Ausforming in a Medium-carbon Bainitic Steel," *Isij Int,* vol. 60, no. 9, pp. 2007-2014, 2020, doi: 10.2355/isijinternational.ISIJINT-2020-054.

[53] B. Liu, W. Li, X. Lu, X. Jia, and X. Jin, "The effect of retained austenite stability on impact-abrasion wear resistance in carbide-free bainitic steels," *Wear,* vol. 428-429, pp. 127-136, 2019, doi: 10.1016/j.wear.2019.02.032.

[54] J. Zhao *et al.*, "Inconsistent effects of austempering time within transformation stasis on monotonic and cyclic deformation behaviors of an ultrahigh silicon carbide-free nanobainite steel," *Materials Science and Engineering: A,* vol. 751, pp. 80-89, 2019, doi: 10.1016/j.msea.2019.01.100.

[55] H. Hu, G. Xu, L. Wang, M.-x. Zhou, and Z.-l. Xue, "Effect of ausforming on the stability of retained austenite in a C-Mn-Si bainitic steel," *Metals and Materials International,* vol. 21, no. 5, pp. 929-935, 2015, doi: 10.1007/s12540-015-5156-5.

[56] M.-x. Zhou, G. Xu, L. Wang, Z.-l. Xue, and H.-j. Hu, "Comprehensive analysis of the dilatation during bainitic transformation under stress," *Metals and Materials International,* vol. 21, no. 6, pp. 985-990, 2015, doi: 10.1007/s12540-015-2348-y.

[57] M. J. Holzweissig, D. Canadinc, and H. J. Maier, "In situ characterization of backstress effects on the austenite-to-bainite phase transformation," *Scripta Materialia,* vol. 67, no. 4, pp. 368-371, 2012, doi: 10.1016/j.scriptamat.2012.05.027.

[58] A. Matsuzaki, H. K. D. H. Bhadeshia, and H. Harada, "Stress affected bainitic transformation in a Fe-C-Si-Mn alloy," *Acta Metallurgica et Materialia,* vol. 42, no. 4, pp. 1081-1090, 1994, doi: 10.1016/0956-7151(94)90125-2.

[59] P. H. Shipway and H. K. D. H. Bhadeshia, "The effect of small stresses on the kinetics of the bainite transformation," *Materials Science and Engineering: A,* vol. 201, no. 1-2, pp. 143-149, 1995, doi: 10.1016/0921-5093(95)09769-4.

[60] M. J. Holzweissig, M. C. Uslu, H. G. Lambers, D. Canadinc, and H. J. Maier, "A Comparative Analysis of Austenite-to-Martensite and Austenite-to-Bainite Phase Transformation Kinetics in Steels," *Materials Research Letters,* vol. 1, no. 3, pp. 141-147, 2013, doi: 10.1080/21663831.2013.798748.

[61] J. G. He, A. M. Zhao, H. Yao, C. Zhi, and F. Q. Zhao, "Effect of Ausforming Temperature on Bainite Transformation of High Carbon Low Alloy Steel," *Materials Science Forum,* vol. 817, pp. 454-459, 2015, doi: 10.4028/www.scientific.net/MSF.817.454.

[62] J. He, A. Zhao, C. Zhi, and H. Fan, "Acceleration of nanobainite transformation by multi-step ausforming process," *Scripta Materialia,* vol. 107, pp. 71-74, 2015, doi: 10.1016/j.scriptamat.2015.05.023.

[63] L. M. Rivas, "Microstructure and mechanical response of nanostructured bainitic steels," *National Center for Metallurgical Research (CENIM-CSIC), Spain,* vol. PhD Thesis, 2016.